BCSJ Award Article

Organic Nanoparticles of Cyanine Dye in Aqueous Solution

Zhong-min Ou, Hiroshi Yao,* and Keisaku Kimura

Graduate School of Material Science, University of Hyogo, 3-2-1 Koto, Kamigori-cho, Ako-gun, Hyogo 678-1297

Received May 24, 2006; E-mail: yao@sci.u-hyogo.ac.jp

Ion-based organic dye nanoparticles ranging from tens to hundreds of nanometers have been prepared in aqueous solution. The synthetic approach is based on "ion-association" (hydrophobic ion-pair formation) in water between the dye cation pseudoisocyanine (PIC) and the anion tetraphenylborate (TPB) or tetrakis(4-fluorophenyl)borate (TFPB) ion. Size tuning of spherical and amorphous PIC nanoparticles was accomplished by varying the molar ratio (ρ) of the loaded anion to the dye cation. Electrophoretic characterization revealed that the increase in surface adsorption of anions onto PIC particles brings about an increase in the negative surface charge density, causing a reduction in the surface tension and the mean size of nanoparticles. We found that the optical absorption properties of the PIC nanoparticles exhibited (i) matrix dependence, that is, the 0–0 band position of the PIC chromophore within similar-sized nanoparticles was dependent on the type of counter anions used, and (ii) size dependence, i.e., the 0–0 band position of the PIC chromophore was dependent on the mean nanoparticle diameter when the particles were prepared using the same counter anion.

For more than a decade, inorganic nanoparticles, such as semiconductor and metal nanoparticles, have attracted a great deal of attention from experimentalists and theoreticians and have been studied extensively. This is due to the fact that such nanoparticles are intermediate in size between single molecules and bulk materials and have interesting physical/chemical properties that are size dependent.[1–5] Organic nanoparticles consisting of small molecules, on the other hand, have not been as well investigated as inorganic nanoparticles probably because of the lack of well-defined synthetic approaches. In organic nanoparticles, weak van der Waals intermolecular and hydrogen-bonding interactions are responsible for the specific electronic/optical properties that are fundamentally different from those of inorganic metals or semiconductors.[6] Taking the diversity and physiological activity of organic molecules into consideration, scientific and technological interest in organic nanoparticle has been clearly increasing.[7–9]

To fabricate organic nanoparticles, a few methods have been applied so far, such as laser ablation,[10] sol–gel method,[11] and the reprecipitation method.[12] In particular, since the first report by Nakanishi and co-workers on the synthesis of organic nanoparticles by using the reprecipitation method, this technique has been widely employed to prepare organic nanoparticles of a wide variety of compounds.[12–18] The reprecipitation method is based on the adjustment of inherent solubility of organic materials by adding electrolytes or organic co-solvents. Despite the simplicity in its operation, it is fraught with difficulties. For instance, organic solvents or surfactants are often used to control the particle size, and the obtained size distributions are relatively broad, which is in stark contrast to those for the well-controlled semiconductor or metal nanoparticles.[15] Since many organic materials are insoluble in water and soluble in organic solvents, aqueous procedures require special formulation techniques to utilize or optimize the physiological or technical action.[19] Therefore, the search for ways to control the size, shape, and the physical/chemical properties of organic nanoparticles in pure aqueous media without using specific organic co-solvents or surfactant is still a challenge and is an important aspect in the development of organic nanoscience.

Meanwhile, we have been interested in supramolecular structures of ionic dye assembly in aqueous solution. We showed that some ionic dyes form characteristic nano-mesoscopic structures, such as strings, sheets, or tubular rods,[20–22] and their geometries are greatly influenced by the counter ions present.[23] On the basis of these studies, we have considered that organic nanostructures involving their shape and size can be controlled by optimizing the interionic interaction. In this article, we demonstrate a simple and versatile method to prepare ion-based organic nanoparticles in aqueous solution by using an ion-association approach.[24] This method utilizes the control of hydrophilicity/hydrophobicity of the ionic material itself via ion-pair formation. No organic solvents or surfactants are needed. We focus on the syntheses of pseudoisocyanine (PIC) dye nanoparticles because the dye assemblies including J-aggregates have served as model systems to study energy or exciton transport.[25–28] The PIC dye cation and the hydrophobic tetraphenylborate (TPB) or tetrakis(4-fluorophenyl)borate (TFPB) anion have been combined to prepare the dye nanoparticles ranging from several tens to hundreds of nanometers in aqueous solution, and a formation mechanism of the nanoparticles along with their optical properties is discussed.

Published on the web February 13, 2007; doi:10.1246/bcsj.80.295

Materials and Methods

Materials. 1,1′-Diethyl-2,2′-cyanine bromide (pseudoisocyanine bromide, PIC-Br; the chemical structure is shown in the inset in Fig. 4a) was purchased from Hayashibara Biochemical Laboratories (Okayama, Japan) and used as received. Sodium tetraphenylborate (NaTPB) and sodium tetrakis(4-fluorophenyl)-borate (NaTFPB) dihydrate were purchased from Sigma-Aldrich and used without further purification. Note that both NaTPB and NaTFPB include hydrophobic TPB and TFPB anions, respectively, which are often used for ion-pair extraction.[29–31] Hence, we expect that ion association between PIC cations and TPB (or TFPB) anions, namely, $(PIC^+ \cdot TPB^-)_m$ or $(PIC^+ \cdot TFPB^-)_m$, leads to water-insoluble nanoparticle formation. Pure water was obtained by using an Aquarius GSR-200 (Advantec Co., Ltd.) water distillation system.

Synthesis of PIC Nanoparticles. At room temperature, rapid addition (<2 s) of 0.5–1.0 mL of aqueous PIC-Br solution (0.1 mM) into an ultrasonicated aqueous solution (2.0–3.0 mL) of NaTPB (0.1 mM), or that (1.0–2.0 mL) of NaTFPB (0.1 mM) produced PIC-based nanoparticles, as confirmed by the fact that the dispersions exhibited the characteristic Tyndall scattering (see Supporting Information). Ultrasonic agitation was further employed for 10 min. Samples prepared by using PIC/TPB and PIC/TFPB are referred to as PIC-**1** and PIC-**2**, respectively.[32] The mean particle size was controlled by changing the molar ratio (ρ) of the loaded NaTPB (or NaTFPB) to PIC-Br.

Instruments. Surface ζ-potential and dynamic light scattering (DLS) measurements of nanoparticles in aqueous solution were conducted with an Otsuka ELS-800 electrophoretic light scattering spectrophotometer with a 10 mW He-Ne laser. For the measurement of ζ-potentials, a constant voltage (80 V) was applied between platinum electrodes in a cuvette cell at room temperature. The cell was washed with a sample dispersion to avoid unintended contamination with spurious species from the cell wall. Since the particles are subject to electroosmotic flow superimposed on their electrophoretic mobility, the measurements were conducted at several different points to separate the intrinsic electrophoretic mobility from the electroosmotic flow. The shapes and sizes of the nanoparticles were observed with a Hitachi-8100 transmission electron microscope (TEM) operated at 200 kV. Selected area electron diffraction patterns were obtained at a camera length of 1 m under the TEM observations. The specimens for TEM observations were prepared by dropping the suspension on an amorphous carbon-coated copper mesh. UV–visible absorption spectra were recorded on a Hitachi U-4100 spectrophotometer. Before the measurements, the samples were freshly prepared and filtered by a 200 nm pore size membrane filter (Sartorious, mini-star RC-15).

Calculation of the Surface Charge Density of Nanoparticles. The surface charge density, σ, is determined by the adsorption of ions onto the particle surface. We, here, assume that the charge of the PIC nanoparticle is located at the solid/solution interface, which is characterized by the electrostatic surface potential φ_0.[33] In a description based on the Poisson–Boltzmann equation for 1–1 electrolytes, σ of an isolated particle with radius R can be expressed in terms of φ_0 as[34]

$$\sigma = \frac{2\varepsilon\varepsilon_0\kappa}{\beta}\left(\sinh\left(\frac{\beta e\varphi_0}{2}\right) + \frac{2}{\kappa R}\tanh\left(\frac{\beta e\varphi_0}{4}\right)\right), \quad (1)$$

where ε or ε_0 is the relative or vacuum dielectric constant, respectively, e is the protonic charge, and $\beta^{-1} = k_B T$ (k_B: Boltzmann constant, T: temperature) is the thermal energy. The Debye length κ^{-1} is expressed as

$$\kappa^{-1} = \sqrt{\frac{\varepsilon\varepsilon_0}{2N_A\beta e^2 I}}, \quad (2)$$

where N_A and I are the Avogadro's number and the ionic strength, respectively.[35]

For calculating σ of PIC nanoparticles by using Eqs. 1 and 2, we used an experimentally derived potential (ζ-potential) instead of a surface potential (φ_0).[34]

Results and Discussion

Size Tuning of PIC Nanoparticles. A series of PIC-**1** or PIC-**2** nanoparticles with different average sizes ranging from about 50 to 130 nm was successfully prepared in aqueous solution by controlling ρ of TPB or TFPB to PIC, respectively. Figures 1a–1c display TEM images of PIC-**1** nanoparticles prepared at $\rho = 2$, 4, 6, respectively, and Figures 1d–1f show those of PIC-**2** nanoparticles prepared at $\rho = 1$, 2, 4, respectively.[36] Spherical particles in the size range of 110–130, 70–90, and 50–70 nm, respectively, for PIC-**1** and those in the range of 100–130, 65–95, and 50–70 nm, respectively, for PIC-**2** were observed. In both systems, the particle size strongly depended on ρ, that is, the mean particle diameter decreased with an increase in ρ. Electron diffraction patterns of PIC-**1** and PIC-**2** nanoparticles show diffusive halos as displayed in the insets of Figs. 1b and 1e, respectively. This confirms that both PIC-**1** and PIC-**2** nanoparticles are amorphous.

DLS measurements were conducted to determine the size distribution of PIC nanoparticles in solution. Figures 2a–2c and 2d–2f show the obtained size distributions of PIC-**1** and PIC-**2** nanoparticles, respectively, in which the polydispersity was less than 15%. The mean diameters are summarized in Table 1. The mean diameter of nanoparticles estimated by DLS agreed well with that obtained by TEM, i.e., DLS characterization also confirmed the size-tunable PIC nanoparticle formation as a function of ρ.

Size Dependence of the Surface Charge Density of PIC Nanoparticles. The PIC-**1** nanoparticle sample prepared at $\rho = 1$ was initially dispersed in solution; however, agglomerates (or precipitates) formed quickly. At $\rho > 1$, that is, excess NaTPB was present in solution, the particles were observed to be stable with no precipitation. A simple measurement of the surface electric property by using a gel electrophoresis showed that the particles were negatively charged.[24] This indicates that the PIC-**1** nanoparticles are electrostatically stabilized by the adsorption of TPB anions. Similar results were obtained for the PIC-**2** nanoparticles; however, we could obtain relatively stable PIC-**2** nanoparticles even when prepared at $\rho = 1$, implying that TFPB anions adsorb more readily onto nanoparticle surfaces than TPB. The size decrease in the PIC nanoparticles with increasing ρ suggests that the adsorption of TPB or TFPB anions onto nanoparticles surfaces suppresses the growth of nanoparticles.

To quantitatively understand the surface charge properties of PIC nanoparticles, we measured their ζ-potentials by using the electrophoretic light scattering method. Figures 3a and 3b show typical electroosmotic profiles of PIC-**1** and PIC-**2** nanoparticles ($\rho = 4$), respectively. A parabolic flow due to the electroosmotic effect influenced the migration of nanoparti-

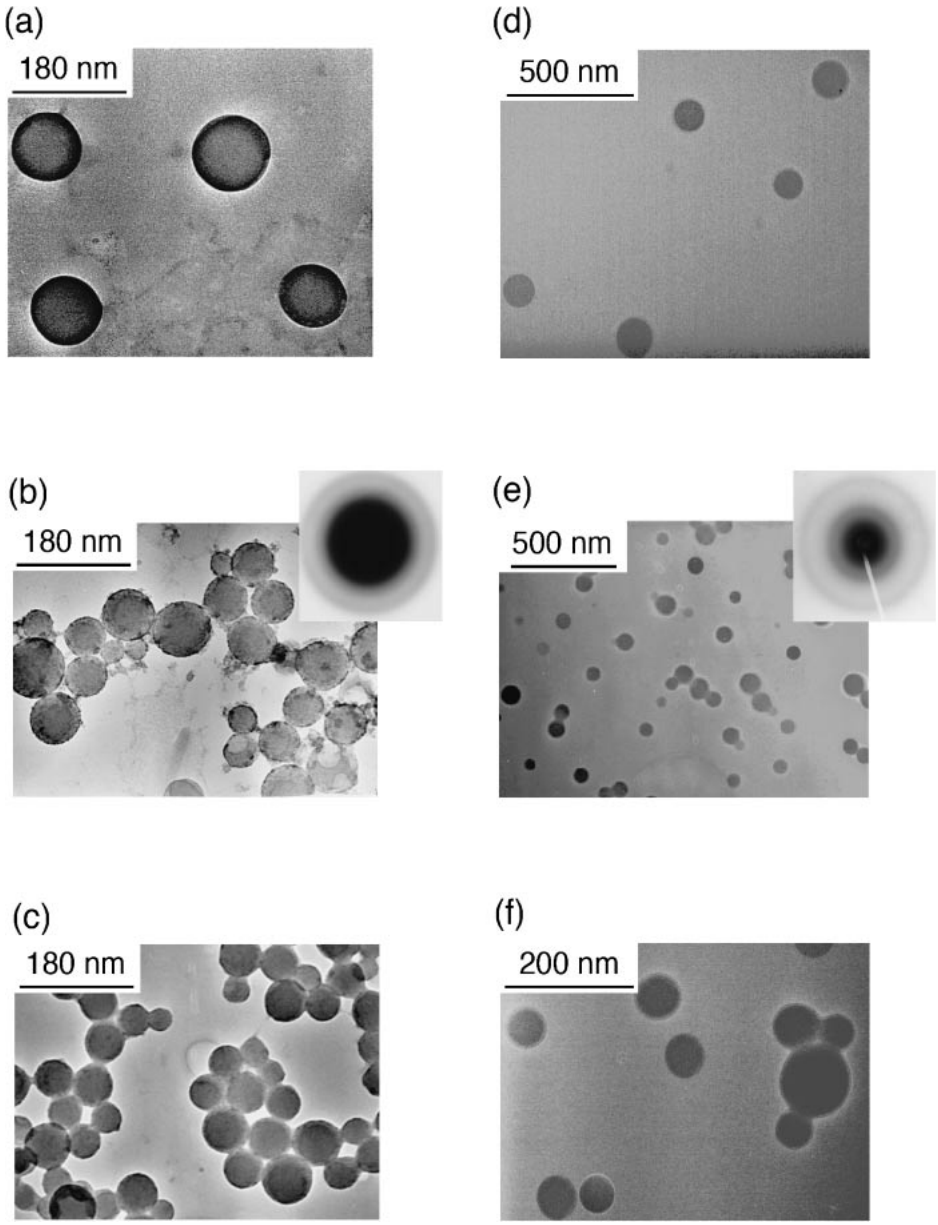

Fig. 1. Representative TEM images of PIC nanoparticles. (a)–(c): PIC-**1** nanoparticles prepared at (a) $\rho = 2$, (b) $\rho = 4$, (c) $\rho = 6$. (d)–(f): PIC-**2** nanoparticles prepared at (d) $\rho = 1$, (e) $\rho = 2$, (f) $\rho = 4$. The insets in (b) and (e) show electron diffraction patterns of the corresponding particles.

cles. We could observe a perfect monotonic peak as a function of the cell position for any of the PIC nanoparticles prepared at different ρ. The result indicates the existence of unique species in the sample dispersion, i.e., there are no other charged states in the sample dispersion. From the profile analyses, the negative ζ-potential and the electrophoretic mobility (μ) could be obtained. Furthermore, we could calculate σ for the PIC nanoparticles from Eqs. 1 and 2.[35] The data are also listed in Table 1. The table shows that the ζ-potential and σ strongly depend on the mean particle diameter.

From Table 1, we can see that the particle size becomes larger with decreasing the absolute value of σ. The phenomenon can be interpreted in terms of the relation between the surface excess of adsorbate and the surface tension.[33] On the basis of Gibbs' adsorption equation as expressed in Eq. 3,[30]

$$\Gamma = -\frac{C}{R_g T}\frac{d\gamma}{dC}, \tag{3}$$

where Γ, C, γ and R_g is the surface excess of adsorbate, solute concentration, surface tension, and the gas constant, respectively, the increase in the surface adsorption of ions, i.e., the increase in Γ accompanied by an increase in C, causes a decrease in γ of the nanoparticles (that is, $d\gamma/dC < 0$), resulting in an decrease in particle size. Under these conditions, the absolute value of σ should increase. This behavior is similar to the case of metal oxide nanoparticles, in which the size decrease is caused by the surface adsorption of ions.[37,38] We can then conclude that the particle size is essentially determined by σ due to the adsorption of univalent TPB or TFPB anions.

Formation Mechanism of PIC Nanoparticles. PIC nano-

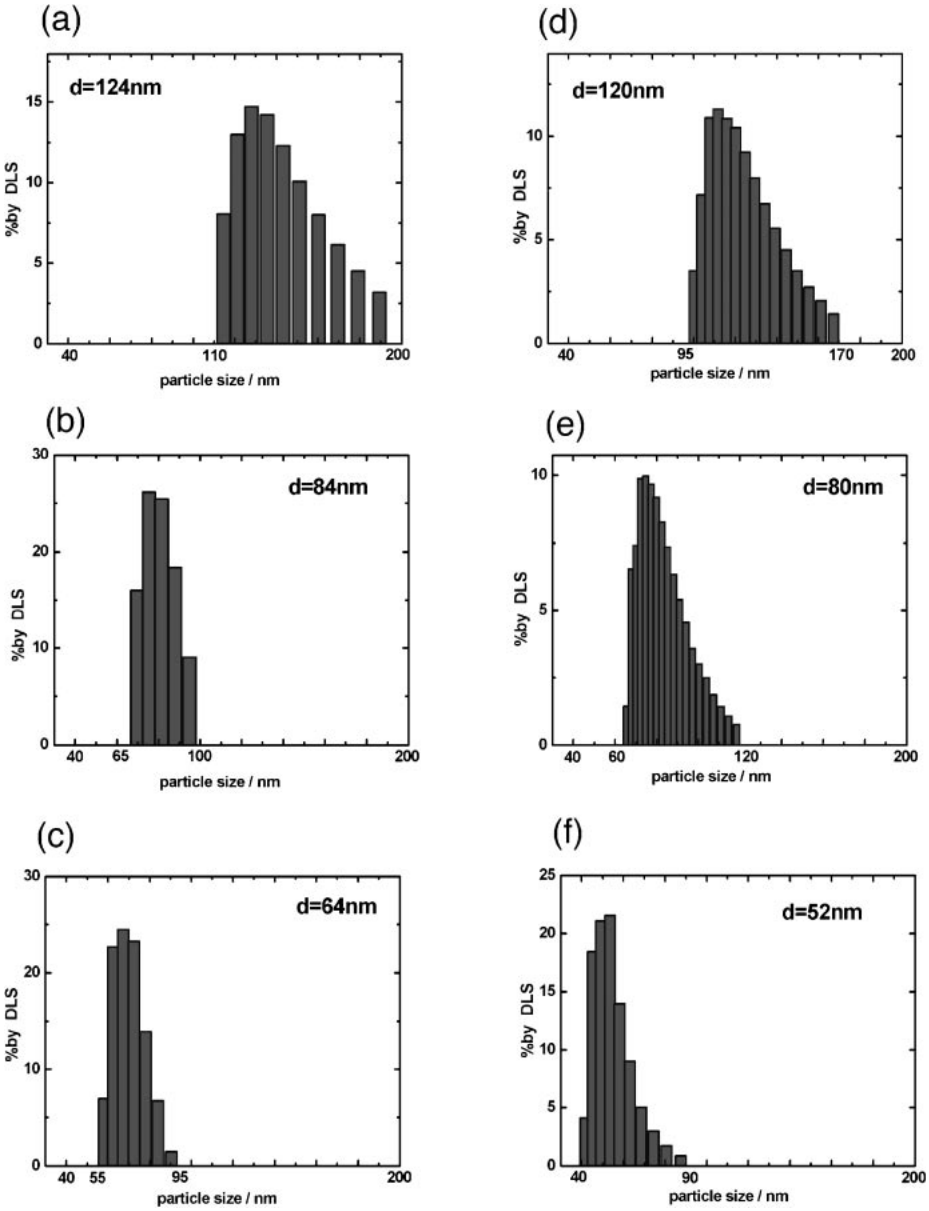

Fig. 2. Particles size distribution of PIC nanoparticles determined by DLS: (a)–(c): PIC-**1** nanoparticles prepared at (a) $\rho = 2$, (b) $\rho = 4$, and (c) $\rho = 6$. (d)–(f): PIC-**2** nanoparticles prepared at (d) $\rho = 1$, (e) $\rho = 2$, (f) $\rho = 4$.

Table 1. Surface Properties of PIC-**1** and PIC-**2** Nanoparticles

	ρ	$\mu/10^{-4}\,\mathrm{cm^2\,V^{-1}\,s^{-1}}$	ζ-Potential/mV	$\sigma/\mathrm{mC\,m^{-2}}$	Mean diameter/nm
	2	−1.98	−26.7	−0.81	124
PIC-**1**	4	−2.44	−33.2	−1.26	84
	6	−3.31	−44.2	−1.96	64
	1	−1.61	−21.9	−0.61	120
PIC-**2**	2	−2.28	−31.6	−1.16	80
	4	−2.26	−36.7	−1.75	52

particles are produced via ion-association reaction between the dye cation and the hydrophobic anion in aqueous solution. Once NaTPB (or NaTFPB) is added into the aqueous PIC-Br solution, TPB^- (or $TFPB^-$) and PIC^+ contact with each other to form an electrically neutral ion-pair because of the strong electrostatic attraction between the oppositely charged ions.[31] The contact ion-pairs will aggregate themselves by van der Waals attractive interaction to produce embryos or nuclei for the particle formation.[19] Note that the TPB (or TFPB) anion does not have a planar structure but rather a tetrahedral structure due to the phenyl rings,[39] so that the growth of nuclei caused by the agglomeration of such contact ion-pairs should

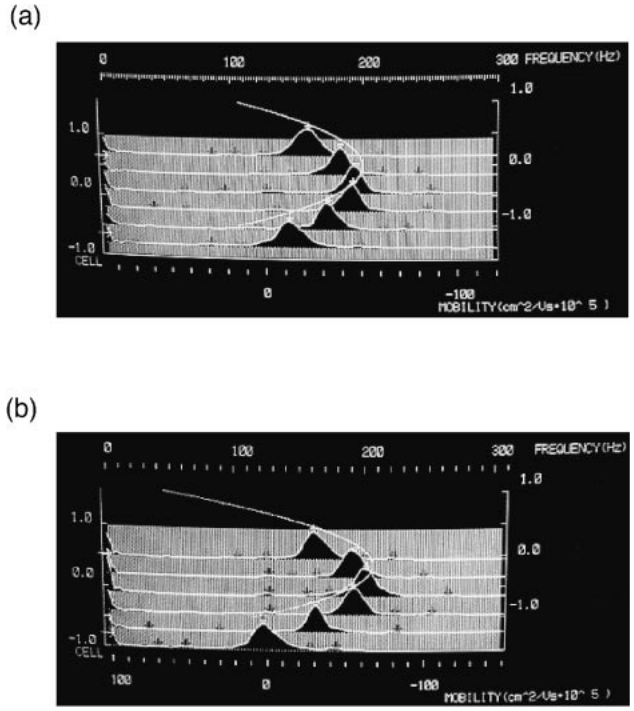

Fig. 3. Photographs of the electroosmotic profile at several different positions from the cell wall. (a) PIC-**1** nanoparticles at $\rho = 4$, (b) PIC-**2** nanoparticles at $\rho = 4$.

lead to spherical nanoparticles. During particle growth, excess anions begin to adsorb on the particle surface probably also due to the van der Waals interaction. The competition between the agglomeration of ion-pairs and adsorption of excess anions would determine the size of nanoparticles. In addition, a large ρ value (or a high ionic strength) increases σ by screening the electrostatic repulsion at the interface, allowing more surface sites to charge up, which contributes to further lowering of the interfacial tension of the system. Under the situation, smaller particles can be formed. A similar mechanism is also found for metal oxide nanoparticles.[37,38]

It is worth noting that, for PIC-**1** nanoparticles, the particle size does not change at $\rho \geq 6$. The fact indicates that TPB adsorption on the particle surface was saturated at $\rho \geq 6$. Similar saturation behavior was also observed for PIC-**2** nanoparticles: TFPB adsorption was saturated at $\rho \geq 4$ since the particle size no longer decreased. According to the obtained σ of each of the PIC nanoparticles in Table 1, saturated adsorption amount (or density) of TPB or TFPB is calculated to be 1-anion per ca. 80 or 90 nm^2, respectively.

Optical Properties of PIC Nanoparticle. Matrix Effect: The UV–vis absorption spectra of PIC-**1** and PIC-**2** nanoparticles with different sizes are shown in Figs. 4a and 4b, respectively. For comparison, the spectrum of PIC-Br monomer solution (0.1 mM) is also shown along with those of PIC-**1** and PIC-**2** nanoparticles with the diameter of ca. 80 nm (Fig. 4c). In Fig. 4c, the spectra were normalized to the maximum absorbance. The spectral shapes of PIC nanoparticles and the monomer exhibited a similar distinct 0–0 absorption band (π–π transition originated from the PIC chromophore) accompanied by two resolved vibronic satellites. This indicates that the PIC chromophore units did not aggregate themselves within nanoparticles, different from J-aggregates (H-aggregates) frequently observed for the dye/anionic-site adsorption systems that show a red-shifted (blue-shifted) and narrow absorption band compared to the monomer absorption band.[23,40–42]

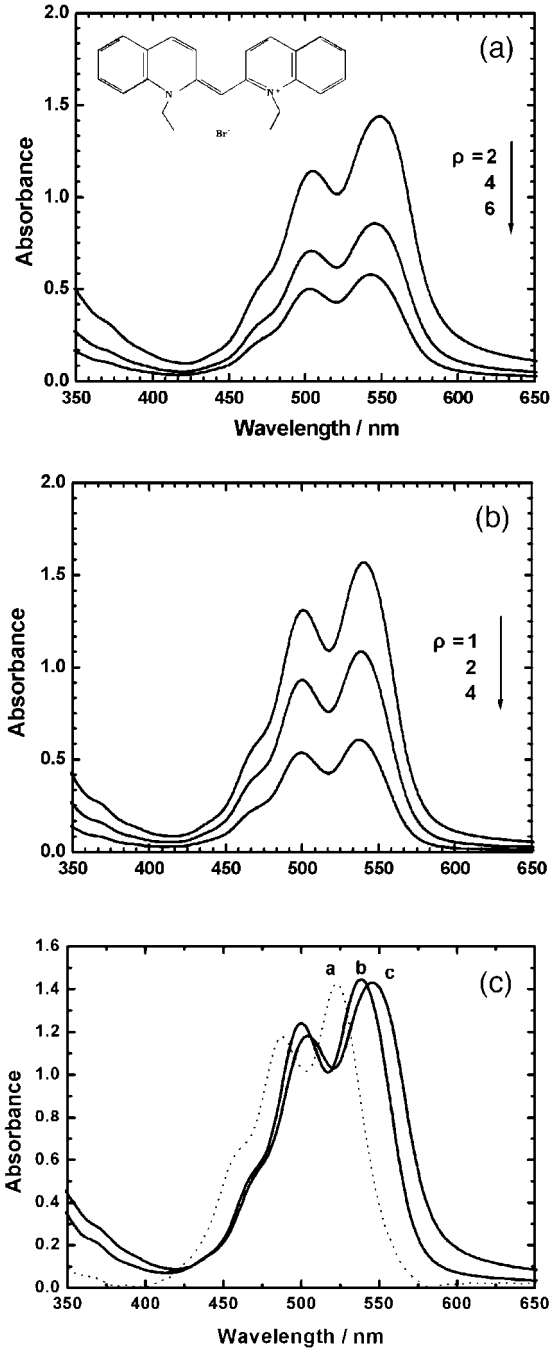

Fig. 4. Absorption spectra of (a) PIC-**1** and (b) PIC-**2** nanoparticles in aqueous solution with different sizes (or different ρ). The inset shows the chemical structure of PIC. (c) Comparison of absorption spectra of similar sized PIC nanoparticles; PIC-**1** (diameter: 84 nm, line **c**) and PIC-**2** nanoparticles (diameter: 80 nm, line **b**). The spectrum of the PIC-Br solution (0.1 mM) is also shown (line **a**).

Moreover, the 0–0 band positions of nanoparticles (both PIC-**1** and PIC-**2**) were significantly red-shifted compared to that of monomer in water (Fig. 4c). Note that the peaks for

PIC-**2** nanoparticles were blue-shifted as compared to those of PIC-**1** nanoparticles. Since it is known that surface charges on a spherical particle smaller than the probe wavelength do not appreciably affect the extinction cross section (i.e., surface charges on a particle scarcely perturb its scattering and absorbing properties),[43] the excess surface charges caused by TPB^- (or $TFPB^-$) adsorption on the particle surface do not palpably influence the optical absorption of PIC nanoparticles. The negative electric fields induced by TPB^- (or $TFPB^-$) within the particle might influence the electronic state of PIC chromophores; however, its contribution would be small because such interaction is "averaged" in an amorphous solid. Hence, the observed red shift from the aqueous monomer peak position can be interpreted in terms of the "matrix (or solvent) effect" that is related to the matrix polarizability. Within a nanoparticle, it is conceivable that PIC is distributed in a TPB (or TFPB) matrix with a high index of refraction due to the abundant phenyl rings, and thus, the red shift of the 0–0 band with respect to the aqueous monomer position is expected. For the PIC dye, a linear relationship has been found between the 0–0 band maximum (ν in cm^{-1}) and the matrix polarizability function $\Phi(n^2) = (n^2 - 1)/(n^2 + 2)$ as follows,[44]

$$\nu \approx 19716 - 2964\Phi(n^2), \tag{4}$$

where n is the refractive index of the matrix for Na-D line at room temperature. The energy of $19716\,cm^{-1}$ corresponds to that of the 0–0 transition of monomeric PIC in a nonsolvated state.[44] Using Eq. 4, for instance, $n = 1.83$ and $n = 1.66$ was obtained for the PIC-**1** (64 nm in diameter) and PIC-**2** (52 nm in diameter) nanoparticle samples, respectively. Matrices having electronegative substituents, such as fluorine, are known to possess lower refractive indices compared to those without them, meaning that the calculated refractive indices are in accordance with those we have expected: The n value of TFPB is lower than that of TPB. Although no n values for TPB (and TFPB) matrices have been published, the estimated n values seem to be reasonable since other organic solids show similar n values; for example, an aromatic anthracene crystal ($n = 1.77$)[45] and amorphous polymer (PPNA) with attached *p*-nitroaniline moieties as side groups ($n = 1.82$)[46] are similar.

It should be noted that PIC monomer is known to be practically non-fluorescence in fluid solvents at room temperature.[47] However, we observed distinct fluorescence from the PIC nanoparticles in solution, quite similar to that of PIC in a solid matrix of polyvinyl alcohol.[47] This result implies that immobilization of PIC in amorphous solid matrices brought about its fluorescence enhancement because of the reduction of nonradiative channels caused by the internal molecular motions. The fact strongly suggests that the PIC is distributed in a hydrophobic TPB or TFPB matrix within the nanoparticles (See Supporting Information for more details).

Size Effect: Also, from Fig. 4, the absorption spectrum of PIC nanoparticles is strongly dependent on the particle size. In Fig. 4a, the 0–0 band of PIC-**1** nanoparticles slightly shifted to shorter wavelength from 549 to 543 nm (energy difference: 24.8 meV) as the average particle diameter decreased from 125 to 64 nm. An energy difference of 12.8 meV was found for the PIC-**2** nanoparticle system when the average particle diameter decreased from 120 to 52 nm (Fig. 4b). The particle size dependence of the 0–0 band position for PIC nanoparticles is shown in Fig. 5. Similar size-dependent phenomena have been reported for perylene and pyrazoline organic nanoparticles,[13,16,48–50] which may not come from so-called quantum confinement because of the small radii of the Frenkel exciton in organic compounds.[8] In our experimental results, the following reasons may be responsible for the size-dependent spectral shift: (i) Mie scattering,[51,52] (ii) influence of the matrix refractive index on the chromophore, (iii) matrix softening. In scheme (i), Mie scattering occurs when an electromagnetic wave interacts with particles with diameters on the order of the wavelength of light, such as the case of our PIC nanoparticles. Actually, Mie scattering can affect the peak position of the absorption spectra, which is often observed for metal nanoparticles.[52]

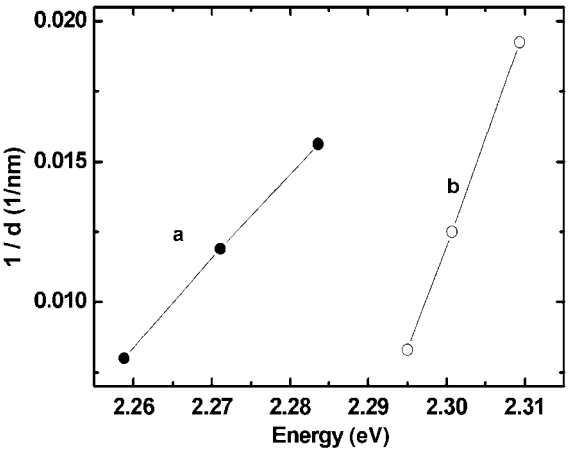

Fig. 5. Relationship between the inverse average particle diameter and the absorption energy of the 0–0 band of PIC chromophore. Lines **a** and **b** correspond to the results of PIC-**1** and PIC-**2** nanoparticles, respectively.

In Fig. 5, an inverse dependence of the particle diameter on the 0–0 absorption peak energy was detected, suggesting that the size-dependent optical properties come from the effect of the surface-to-volume ratio. In scheme (ii), the electronic state of chromophores in the vicinity of the nanoparticle surface can be affected by the surrounding water. From a statistical point of view, the effective refractive index of the matrices may then depend on the size (or surface-to-volume ratio) of the nanoparticles, yielding the relevant spectral shifts. In scheme (iii), matrix softening would be brought about by a surface distortion caused by the increase in the surface-to-volume ratio, causing the change in interionic interactions.[14,19,48] Hence, we believe that contributions from the schemes (ii) and/or (iii) are significant to the observed size effect.

It is worth noting that the different size effect were observed between PIC-**1** and PIC-**2** nanoparticle systems. In Fig. 5, the slope for PIC-**2** nanoparticles was steeper than that for PIC-**1**. This intriguing result indicates that ion-based organic nanoparticles can have different size dependence of their spectroscopic properties when different associative counter ions (or matrices) are used to prepare the nanoparticles having identical chromophores. In other words, the optical and structural parameters of ion-based organic nanoparticles are highly controllable. In conclusion, our procedure offers the possibility of a general-

ized approach to the production of advanced ion-based organic nanoparticles with size tunability, so that synthesis of different ion-based organic nanoparticles is underway in our laboratory.

Conclusion

Spherical and amorphous nanoparticles of organic pseudoisocyanine (PIC) dye were prepared by using an "ion-association method" in aqueous solution. The approach is based on ion-pair formation between the PIC cation and the TPB or TFPB anion, which gives rise to a hydrophobic phase in water. For preparation, neither surfactant nor organic co-solvent was involved. The size of the PIC nanoparticles could be controlled by adjusting the interionic interaction between the dye cation and the associative hydrophobic counter anion. The increase in surface adsorption of TPB (or TFPB) ions brought about the increase in the surface charge density, causing a reduction in the interfacial tension and the size of the nanoparticles. A formation mechanism for the nanoparticles was proposed in terms of the competition between the aggregation of contact ion-pairs and the surface adsorption of excess anions present in aqueous solution. We also found the matrix and size dependence of spectroscopic properties of PIC nanoparticles. We expect that this technique, a simple size-tunable method, will play a vital role in the versatile syntheses of various ion-based organic nanoparticles in the future.

A part of this work was financially supported by Grant from Kawanishi Memorial Shinmeiwa Education Foundation and Grant-in-Aids for Scientific Research (S: 16101003, from MEXT).

Supporting Information

Photos of the PIC-**1** nanoparticle suspension showing the Tyndall scattering effect, FT-IR spectra of the precipitated PIC nanoparticles, and the fluorescence properties of the nanoparticle samples.

References

1 A. P. Alivisatos, *Science* **1996**, *271*, 933.
2 M. Bruchez, Jr., M. Moronne, P. Gin, S. Weiss, A. P. Alivisatos, *Science* **1998**, *281*, 2013.
3 X. Peng, L. Manna, W. Yang, J. Wickham, E. Scher, A. Kadavanich, A. P. Alivisatos, *Nature* **2000**, *404*, 59.
4 J. S. Yin, Z. L. Wang, *Phys. Rev. Lett.* **1997**, *79*, 2570.
5 S. H. Wang, H. Yao, S. Sato, K. Kimura, *J. Am. Chem. Soc.* **2004**, *126*, 7438.
6 E. A. Silinsh, *Organic Molecular Crystals: Their Electronic States*, ed. by M. Cardona, P. Fulde, H. J. Queisser, Springer-Verlag, Berlin, **1980**, Chap. 1.
7 T. Uemura, S. Kitagawa, *J. Am. Chem. Soc.* **2003**, *125*, 7814.
8 D. Xiao, L. Xi, W. Yang, H. Fu, Z. Shuai, Y. Fang, J. Yao, *J. Am. Chem. Soc.* **2003**, *125*, 6740.
9 X. Gong, T. Milic, C. Xu, J. D. Batteas, C. M. Drain, *J. Am. Chem. Soc.* **2002**, *124*, 14290.
10 T. Sugiyama, T. Asahi, H. Masuhara, *Chem. Lett.* **2004**, *33*, 724.
11 A. Ibanez, S. Maximov, A. Guin, C. Chaillout, P. L. Baldeck, *Adv. Mater.* **1998**, *10*, 1540.
12 H. Kasai, H. S. Nalwa, H. Oikawa, S. Okada, H. Matsuda, N. Minami, A. Kakuta, K. Ono, A. Mukoh, H. Nakanishi, *Jpn. J. Appl. Phys., Part 2* **1992**, *31*, L1132.
13 H. Kasai, H. Kamatani, Y. Yoshikawa, S. Okada, H. Oikawa, A. Watanabe, O. Itoh, H. Nakanishi, *Chem. Lett.* **1997**, 1181.
14 B. K. An, S. K. Kwon, S. D. Jung, S. Y. Park, *J. Am. Chem. Soc.* **2002**, *124*, 14410.
15 A. J. Gesquiere, T. Uwada, T. Asahi, H. Masuhara, P. F. Barbara, *Nano Lett.* **2005**, *5*, 1321.
16 H. B. Fu, J. N. Yao, *J. Am. Chem. Soc.* **2001**, *123*, 1434.
17 Z. Jia, D. Xiao, W. Yang, Y. Ma, J. Yao, Z. Liu, *J. Membr. Sci.* **2004**, *241*, 387.
18 H. Kamatani, H. Kasai, S. Okada, H. Matsuda, H. Oikawa, N. Mitani, A. Kakuta, K. Ono, A. Mukoh, H. Nakanishi, *Mol. Cryst. Liq. Cryst.* **1994**, *252*, 233.
19 D. Horn, J. Rieger, *Angew. Chem., Int. Ed.* **2001**, *40*, 4330.
20 H. Yao, M. Omizo, N. Kitamura, *Chem. Commun.* **2000**, 739.
21 H. Yao, Y. Kagoshima, S. Kitamura, T. Isohashi, Y. Ozawa, K. Kimura, *Langmuir* **2003**, *19*, 8882.
22 H. Yao, C. A. Michaels, S. J. Stranick, T. Isohashi, K. Kimura, *Lett. Org. Chem.* **2004**, *1*, 280.
23 H. Yao, S. Kitamura, K. Kimura, *Phys. Chem. Chem. Phys.* **2001**, *3*, 4560.
24 H. Yao, Z. Ou, K. Kimura, *Chem. Lett.* **2005**, *34*, 1108.
25 H. Yao, S. Sugiyama, R. Kawabata, H. Ikeda, O. Matsuoka, S. Yamamoto, N. Kitamura, *J. Phys. Chem. B* **1999**, *103*, 4452.
26 S. S. Ono, H. Yao, O. Matsuoka, R. Kawabata, N. Kitamura, S. Yamamoto, *J. Phys. Chem. B* **1999**, *103*, 6909.
27 S. Sugiyama, H. Yao, O. Matsuoka, R. Kawabata, N. Kitamura, S. Yamamoto, *Chem. Lett.* **1999**, 37.
28 H. Yao, Z. Ou, K. Kimura, *Colloids Surf., A* **2004**, *236*, 31.
29 J. Rydberg, M. Cox, C. Musikas, G. R. Choppin, *Solvent Extraction Principle and Practice*, Marcel Dekker Inc., New York, **2004**, pp. 162–166.
30 G. J. Moody, R. K. Owusu, A. M. Z. Slawin, N. Spencer, J. F. Stoddart, J. D. Ronald Thomas, D. J. Williams, *Angew. Chem., Int. Ed. Engl.* **1987**, *26*, 890.
31 X. Yang, A. Zaitsev, B. Sauerwein, S. Murphy, G. B. Schuster, *J. Am. Chem. Soc.* **1992**, *114*, 793.
32 Precisely, the PIC-**1** (PIC-**2**) nanoparticle is composed of PIC and TPB (TFPB) moieties. We verified the binary components by measuring the FT-IR spectra of the precipitated sample. See Supporting Information. In the main text, both of these nanoparticles are called PIC nanoparticles, because their optical properties are dominated by the PIC chromophore.
33 R. J. Hunter, *Foundations of Colloid Science*, Clarendon, Oxford, **1991**, Vol. 1, Chap. 2, pp. 250–255; Chap. 6, pp. 332–337; Vol. 2. Chap. 12, pp. 718–727.
34 S. H. Behrens, D. I. Christl, R. Emmerzael, P. Schurtenberger, M. Borkovec, *Langmuir* **2000**, *16*, 2566.
35 The ionic strength (I) of the solution is given by $I = 0.5\,\Sigma(C_i z_i^2)$, where C_i and z_i are the concentration and valency of ion "i," respectively, and the summation is taken over all the ions in solution. To prepare PIC-**1** nanoparticles under the condition of $\rho = 2$, for instance, 0.1 mL of a PIC-Br aqueous solution (0.1 mM) was added into 0.2 mL of a NaTPB aqueous solution (0.1 mM). We assume that 1–1 ion-pair formation of PIC-TPB produces electrically neutral species, such that free ionic species in the solution are unreacted Na^+, Br^-, and TPB^-. Hence, we can estimate the concentration of each ion in solution as follows;

$C_{Na} = 0.1 \times (2/3) = 1/15\,mM$, $C_{Br} = 0.1 \times (1/3) = 1/30\,mM$, $C_{TPB} = 0.1 \times (1/3) = 1/30\,mM$. Thus, $I = 2/3 \times 10^{-4}$.

36 Although the number of particles is relatively small in each TEM image, similar results could be repeatedly obtained irrespective of the observation areas.

37 L. Vayssieres, A. Hagfeldt, S. E. Lindquist, *Pure Appl. Chem.* **2000**, *72*, 47.

38 L. Vayssieres, N. Beermann, S. E. Lindquist, A. Hagfeldt, *Chem. Mater.* **2001**, *13*, 233.

39 G. R. Desiraju, T. Steiner, *The Weak Hydrogen Bond*, Oxford, New York, **1999**, Chap. 3, pp. 139–145.

40 D. Möbius, *Adv. Mater.* **1995**, *7*, 437.

41 H. Yao, Y. Morita, K. Kimura, *Surf. Sci.* **2003**, *546*, 97.

42 H. Yao, K. Domoto, T. Isohashi, K. Kimura, *Langmuir* **2005**, *21*, 1067.

43 C. R. Bohren, D. R. Huffman, *Absorption and Scattering of Light by Small Particles*, John Wiley & Sons, New York, **1983**, Chap. 4, pp. 116–121.

44 I. Renge, U. P. Wild, *J. Phys. Chem. A* **1997**, *101*, 7977.

45 K. S. Sundarajan, *Z. Kristallogr.* **1936**, *93*, 238.

46 E. Eich, A. Sen, H. Looser, G. C. Bjorklund, J. D. Swalen, R. Twieg, D. Y. Yoon, *J. Appl. Phys.* **1989**, *66*, 2559.

47 H.-P. Dorn, A. Müller, *Chem. Phys. Lett.* **1986**, *130*, 426.

48 H. Kasai, H. Kamatani, S. Okada, H. Oikawa, H. Matsuda, H. Nakanishi, *Jpn. J. Appl. Phys.* **1996**, *35*, L221.

49 S. R. Forrest, *Chem. Rev.* **1997**, *97*, 1793.

50 H. B. Fu, B. H. Loo, D. B. Xiao, R. M. Xie, X. H. Ji, J. N. Yao, B. W. Zhang, L. Q. Zhang, *Angew. Chem., Int. Ed.* **2002**, *41*, 962.

51 V. Volkov, T. Asahi, H. Masuhara, A. Masuhara, H. Kasai, H. Oikawa, A. Nakanishi, *J. Phys. Chem. B* **2004**, *108*, 7674.

52 M. A. van Dijk, A. L. Tchebotareva, M. Orrit, M. Lippitz, S. Berciaud, D. Lasne, L. Cognet, B. Lounis, *Phys. Chem. Chem. Phys.* **2006**, *8*, 3486.